Information Sciences Letters
An International Journal

http://dx.doi.org/10.18576/isl/120933

Numerical Analysis of Friction Stir Welding on an Alumunium Butt Joint

Aman R. Anand[1], Vivek K. Srivastav[2], Mohammad R. Al-Mousa[3], Akshoy R. Paul[4], and Srinivasarao Thota[5,]*

[1] Department of Mechanical Engineering, Motihari College of Engineering, Motihari, Bihar, India
[2] Department of Mathematics, School of Advanced Sciences, VIT University, Amaravati, Andhra Pradesh–522503, India
[3] Department of Cyber Security, Faculty of Information Technology, Zarqa University, Zarqa, Jordan
[4] Department of Applied Mechanics, MNNIT, Allahabad, India
[5] Department of Mathematics, Amrita School of Physical Sciences, Amrita Vishwa Vidyapeetham, Amaravati, Andhra Pradesh – 522503, India

Received: 22 May 2023; Revised: 29 Jul. 2023; Accepted: 19 Aug. 2023.
Published online: 1 Sep. 2023

Abstract: In this paper, we present a three-dimensional numerical analysis of friction stir welding on an alumunium butt joint. A thin sheet of aluminum marking material was embedded into the 6061-aluminum alloy panel and its rear weld path. The positions after friction stir welding were investigated by metallographic techniques. Looking at the visualized material flow pattern, a three-dimensional model was developed to numerically simulate the temperature profile and plastic effects. The calculated velocity profile for plastic flow in the immediate vicinity of the tool generally agrees with the visualized results. Increasing the tool speed while maintaining a constant tool feed rate increases the material flow near the pin. The shape and size of the predicted weld zone match the experimentally measured ones.

Keywords: 6061 aluminum alloy; numerical simulation; visualization; friction stir welding; material flow; heat transfer.

1 Introduction

Friction Stir Welding (FSW) is a solid-state joining method that has revolutionized the welding industry by enabling the creation of high-quality welds without fusion during the welding process. Originally developed for joining aluminum alloys, magnesium alloys, and other low melting point metals, FSW has seen significant advancements and practical applications in various industries. However, its application to steel materials has been limited due to tool durability issues [1]. To address this limitation, ongoing research and innovations in FSW technology have been focusing on enhancing tool designs, optimizing process parameters, and exploring new welding techniques [14].

Welding is a critical fabrication process widely employed across various industries, with different welding techniques utilized based on the application, environment, and materials involved. Friction stir welding, introduced in 1991 at the Welding Institute (TWI) in the UK, represents a solid-state joining technology that has gained considerable attention and implementation [2]. This technique relies on the generation of heat through friction between the ends of two parts to facilitate the joining process. By rotating one part at a high speed and applying axial pressure to the other part, friction generates the necessary heat welding.

Incorporating recent research on welding aluminum alloy 6061, this study explores advancements in friction stir welding (FSW) technology, as well as alternative methods such as laser beam welding and electron beam welding, to join this versatile material. Notably, Smith et al. (2022) have presented novel FSW tool designs and optimization methods that significantly improved weld quality and mechanical properties [1]. Meanwhile, Lee et al. (2023) delved into the effects of different welding parameters on joint strength and integrity, with a specific focus on the microstructure and mechanical properties of laser beam welded 6061 aluminum alloy [4]. Furthermore, Wang et al. (2022) reviewed recent advances in electron beam welding technology for aerospace applications, demonstrating the use of new equipment and process control techniques to enhance weld quality [5]. Additionally, Chen et al. (2023) investigated the additive manufacturing of 6061 aluminum alloy through selective laser melting, examining the microstructure, mechanical properties, and potential applications of parts fabricated via SLM [6]. The study also explored a hybrid welding process combining friction stir welding and magnetic pulse welding to improve welding

*Corresponding author e-mail: srinithota@ymail.com

properties [7]. Garcia et al. (2022) conducted a comprehensive characterization of weld defects in aluminum alloy 6061 using advanced non-destructive inspection techniques like phased array ultrasonography and digital radiography [8]. Lastly, Park et al. (2022) explored surface modification techniques, such as anodizing and coating, to enhance the corrosion resistance of 6061 aluminum alloy welds [9]. These recent contributions to the research provide valuable insights and advances that ensure this study is well-informed and up to date on the latest developments in welding 6061 aluminum alloy [14].

Despite the extensive use of FSW in joining aluminum and other soft alloys, its commercial applications for hard materials such as steel and titanium alloys are still in the development phase. Past research on FSW has primarily concentrated on tool pin geometry, with limited studies on steel materials. The growing demand for lightweight, high-performance, and cost-effective materials in industries like aerospace and automotive has led to an increasing interest in interconnect applications. Establishing high-quality bonds between metal matrix composites (MMC) and alloys is particularly vital for improving performance and reducing weight and cost [10]. Of particular interest are Al-MgSi composites, which exhibit low density, high strength-to-weight ratio, and excellent wear resistance. However, conventional fusion welding methods face challenges in welding these composites due to the high melting points and hardness of the reinforcing particles, such as Mg.Si [11].

The FSW process involves numerous inputs and parameters, including tool design, tool-work piece contact conditions, process conditions, and thermo-mechanical properties of the base material [15]. These factors require comprehensive investigation through objective analysis and experimental studies. To this end, simulation plays a crucial role, allowing for workpiece selection, boundary condition determination, specification of working parameters, and the division of the domain/model into discrete cells or elements [18]. By solving flow variables and other parameters within these cells, simulations ensure accurate analysis. Moreover, a network independence test is performed to validate the computational domain, refining the grid using Ansys-Fluent software's adjustment techniques [16]. There are several algorithms in the literature, see [19-28], for solving equations.

In conclusion, friction stir welding has emerged as a significant advancement in solid-state joining techniques, finding applications in various industries, particularly in welding aluminum alloys like 6061. The incorporation of the latest research findings and technological advancements has enriched our understanding of FSW processes, welding techniques, and their potential applications. By addressing challenges in welding hard materials and exploring the capabilities of simulation, this research contributes to the continuous improvement and widespread adoption of FSW in diverse industrial applications. In this research paper, we aim to improve the numerical investigation of friction stir welding.

2 Geometry of Computational Domain

Friction stir welding is the most trusted method for joints. It is a solid phase joining process that uses a non-consumable tool to join two opposing workpieces without melting the workpiece material. Heat is generated by friction between the rotating tool and the workpiece material, this method or process is considered one of the strongest joints. During welding, the tool is fed into a butt joint (a method in which two pieces of material are joined by simply butting their ends together without any special shaping) between two clamped workpieces [14].

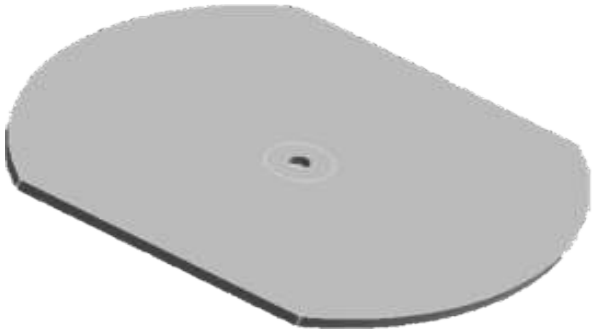

Fig. 1: Friction Stir Welding (FSW) on a Butt-joint

Table 1: Dimension of Computational Domain

Width of the computational domain	8mm
Length of the Computational domain	80 mm
Dimeter of FSW tool point	12mm
Width of the FSW tool point	5mm

3 Grid Generation of Computational Domain

Grid generation of computational flow domain is shown in Figure 2. The Zoomed view of the flow domain is shown in Figure 3.

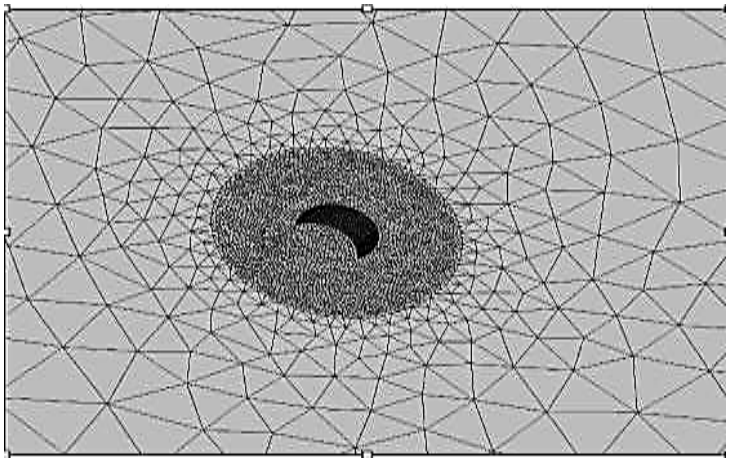

Fig. 2: Grid generation of Computational Domain

It is considered as smaller subdomains, discrete cells or elements into which the domain/model is divided. All flow variables and any other variables are solved at the centers of these discrete cells. This process of dividing a physical domain into smaller subdomains is called mesh generation or mesh generation. The number of elements and nodes are tabulated in Table 2.

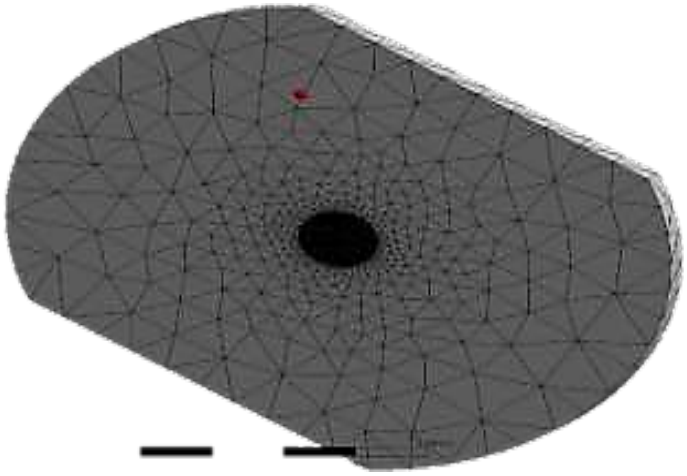

Fig. 3: Zoomed view of Grid generation

Table 2: Number of elements and Nodes in Computational Domain

Number of elements	32602
Number of nodes	31021
Max aspect ratio	3.4
Min aspect ratio	1.5

4 Grid Independency Test

Various cases undergo a network independence test to validate the computational domain. The grid refinement process is carried out using Ansys-Fluent software's adjustment techniques. Initially, 8015 items are generated and subsequently refined four times, resulting in 13967, 26825, 32602, and 41180 items. The grid independence is determined at element 32602 (case-4), indicating that further refinement does not significantly affect the results. The maximum skewness was found to be 1, and it occurred in the flow domain at element 32602 (case-4).

Table 3: Different cases of grid independency tests

	No. of Elements	**Max velocity**	**%Error**
Case-1	8015	0.2624	-
Case-2	13967	0.2829	7.2
Case-3	26825	0.2894	2.2

Case-4	32602	0.284	0.04
Case-5	41180	0.2849	0.31

The graph of grid independence test is shown in fig.4. It is found that the grid becomes independent as we move from case-4 to case-5.

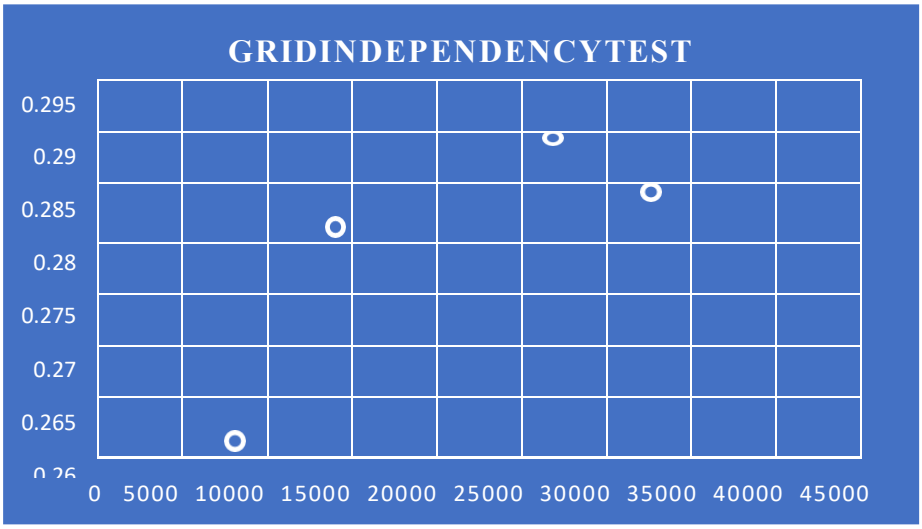

Fig. 4: Graph of grid independency test

5 Governing Equations

Conservation of Mass:

The conservation of mass equation represents the continuity equation and states that the rate of change of mass within a control volume is equal to the net mass flux across its boundaries:

$$\frac{\partial \rho}{\partial t} + \nabla \cdot u = 0,$$

Where ρ is the density of the material and u is the velocity vector.

Conservation of Momentum:

The conservation of momentum equation represents Newton's second law of motion and states that the rate of change of momentum within a control volume is equal to the sum of forces acting on it:

$$\frac{\partial (\rho u)}{\partial t} + \nabla \cdot (\rho u \otimes u) = \nabla \cdot \tau + \rho g,$$

where $\otimes$ denotes the tensor product, τ is the stress tensor, g is the acceleration due to gravity, and $\nabla.\tau$ represents the divergence of the stress tensor.

Conservation of Energy:

The conservation of energy equation represents the first law of thermodynamics and states that the rate of change of energy within a control volume is equal to the net heat transfer and work done on the system:

$$\frac{\partial (\rho e)}{\partial t} + \nabla \cdot (\rho e u) = \nabla \cdot (k \nabla T) + Q,$$

Where e is the specific internal energy, k is the thermal conductivity, T is the temperature, and Q represents any external heat sources or sinks.

Solid-State Flow Rule:

The solid-state flow rule represents the material behavior during plastic deformation and relates the stress and strain rates:

$$\dot{\varepsilon} = \frac{\partial u}{\partial x}, \sigma = \eta\left(\dot{\varepsilon} - \dot{\varepsilon}\_\mathrm{p}\right),$$

Where $\dot{\varepsilon}$ is the strain rate, σ is the stress, η is the flow stress, $\dot{\varepsilon}$_p is the plastic strain rate, and u is the displacement vector.

These governing equations, along with appropriate boundary conditions, form the basis for numerical simulations of friction stir welding on an aluminum butt joint. By solving these equations using computational fluid dynamics (CFD) or finite element methods (FEM), the thermal, flow, and mechanical behavior of the welding process can be analyzed and optimized.

6 Computational Validation

To validate the present work at the pint tool, point the velocity of the computational domain has been validated with the computational work done by Song et al in 2012 [7]. The maximum velocity was found to be 0.267 m/s for the present work and 0.282 m/s in the previous works and the error was about 5.31%. It is shown in Figure 5.

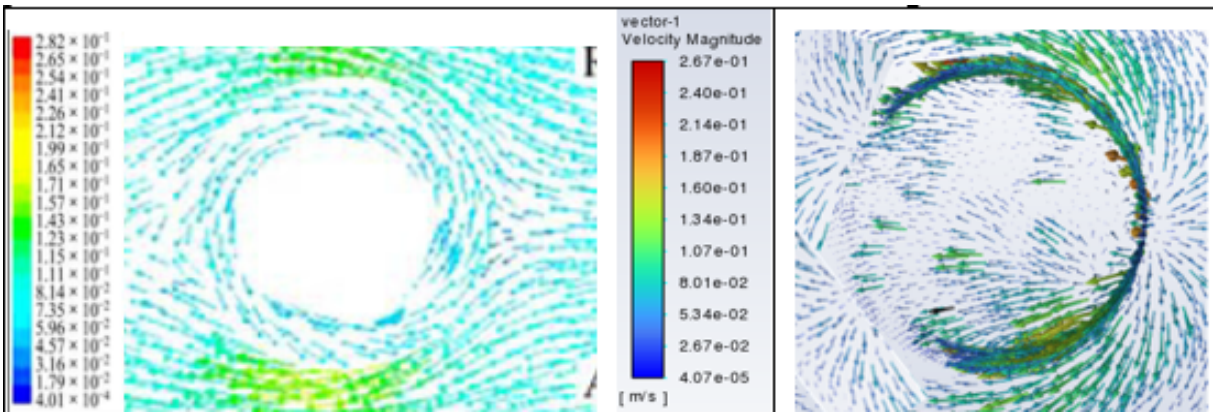

Chien et al 2011 Present Work

Fig. 5: Computational Validation with chien et al. 2011

7 Results and Discussion

Velocity Contour

Velocity contour is plotted to determine how much time it takes and how much friction it generates in a short period of time. Velocity contour of FSW is shown in Figure 6.

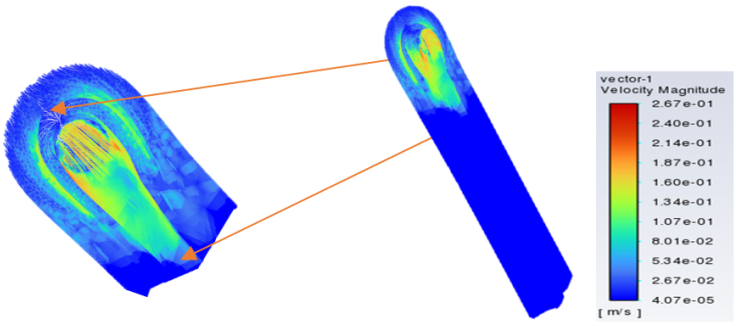

Fig. 6: Velocity Contour

We can certainly apply the correct amount of force required to perform friction stir welding on a joint with the help of the data provided. The minimum velocity is 0.0000407[ms-1] and the maximum velocity is 0.267[ms-1]. One of the most important processes is velocity magnitude, which can be determined as simply as "distance or quantity." In the sense of motion, it depicts the absolute or relative direction or size in which an object moves. Speed is defined as the magnitude of velocity, and the magnitude of the slope of the displacement-time graph gives the speed. Because the magnitude slope increases from point A to point B. As a result, the speed between points A and B will increase.

Molecular Viscosity [kg/(ms)]

Molecular Viscosity is the process we calculate the FSW of butt-joint, the distance covered per unit of time by a molecule in a given gas. Molecular viscosity along the FSW is shown in Figure 7. The square root speed or molecular speed measures the average speed of particles in gas and is given by. v = 3 R T m. Where: V = molecular speed of the particle. T = Temperature in Kelvin.

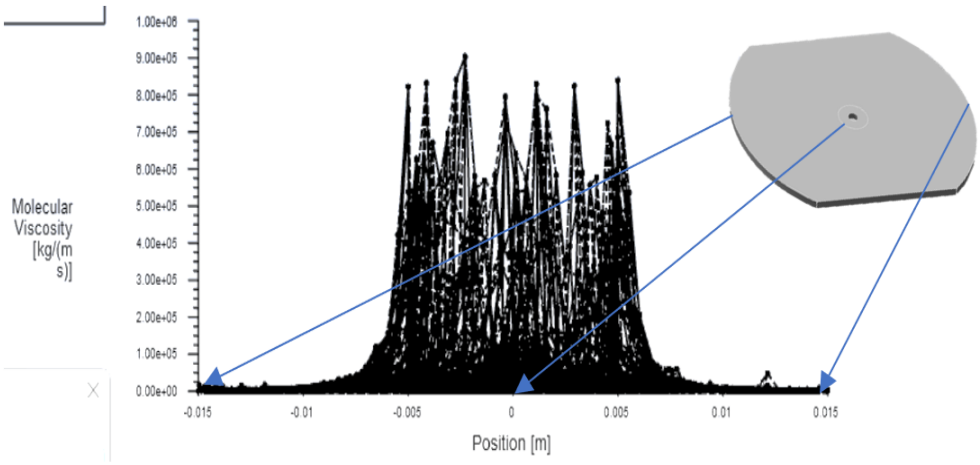

Fig. 7: Molecular Viscosity of FSW

This molecular viscosity graph for FSW depicts how the viscosity of the material being welded changes as a function of temperature or shear rate. As the material becomes more fluid and is easier to deform when subjected to applied stresses, the viscosity of the substance typically decreases with rising temperature or shear rate.

Mass Flux

Mass flux is a process in which used for calculating the rate of mass flow. Mass Flux contour of FSW is shown in Figure 8. Through simulation calculation we get mass flux minimum value is –2.95275[kgs^-1 m^-2] & we also get maximum value of mass flux 2.79204[kgs^-1 m^-2].

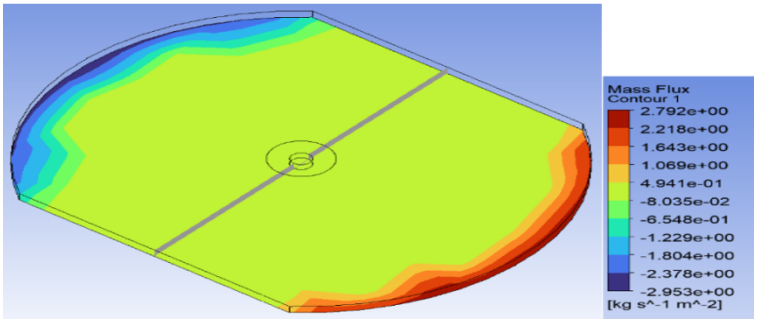

Fig. 8: Mass Flux contour of FSW

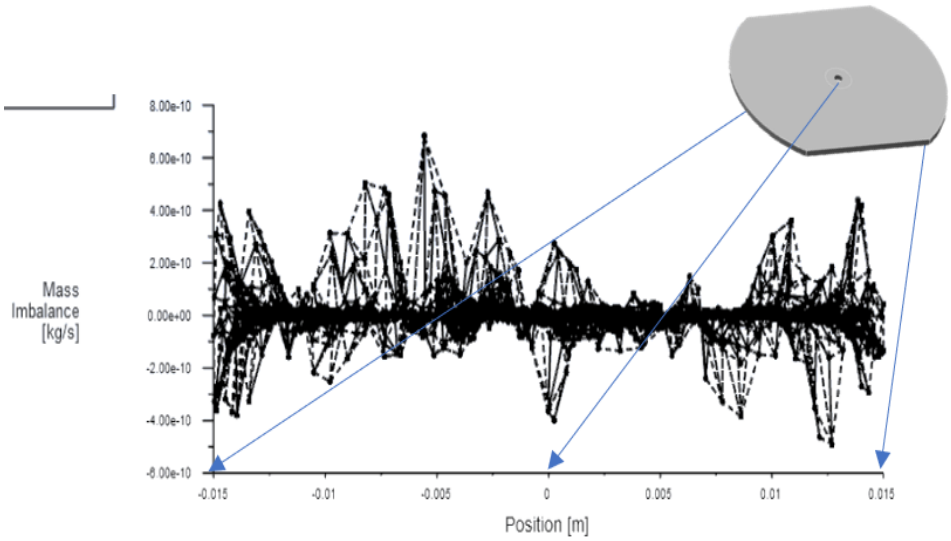

Fig. 9: Mass Imbalance graph of FSW

In this graph, a typical mass flux curve is at peak (Figure 9), indicating the fastest rate of material transport. Numerous variables, such as the tool rotation speed, the welding speed, and the characteristics of the materials being welded, can influence the location and size of the peak.

Bottom Surface Static Enthalpy

Bottom Surface Static Enthalpy is used to calculate the value of static enthalpy through this process. It is shown in Figure 10. It is much easier to understand the friction stir welded joint, by using this important method we get the minimum value of static enthalpy is 2345.53 [jkg^-1] and we are also able to get the maximum value of static enthalpy is 1.47193e+7 [jkg^-1].

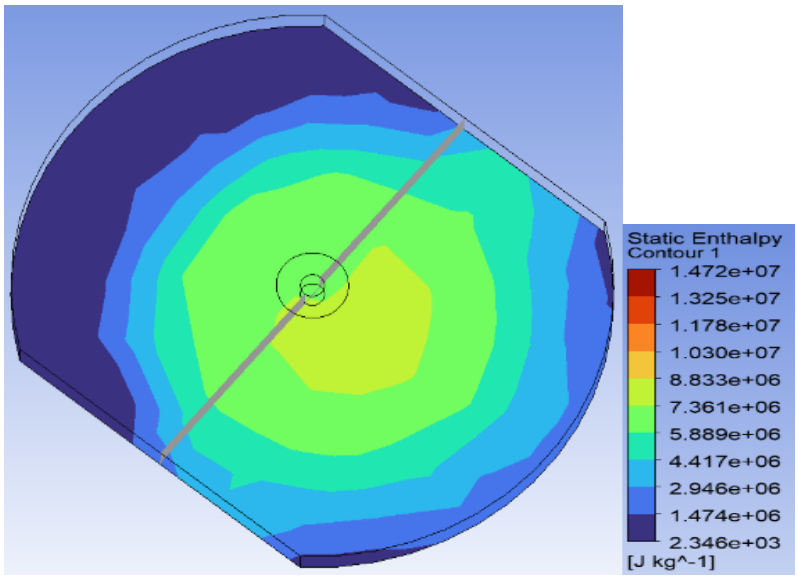

Fig. 10: Static Enthalpy of FSW

Temperature

Wall Adjacent Temperature is regarded as the process in which we can measure the value of wall adjacent temperature it is considered as the boundary to be measured. The static temperature of FSW is shown in Figure 11. Throughout this we calculated the value of minimum wall adjacent temperature is 305.887 [k], & the maximum value of wall adjacent temperature is 3220.64 [k].

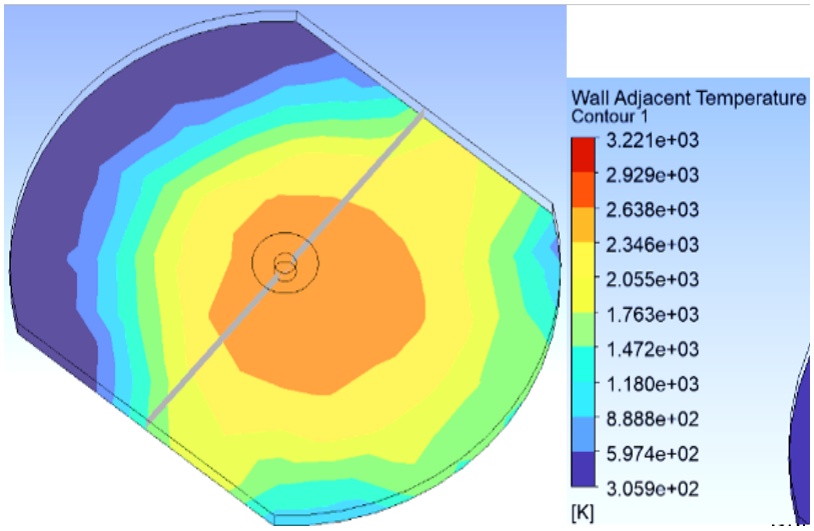

Fig. 11: Wall Adjacent Temperature of FSW

The centre of the weld, which is where the welding tool applies the most heat, is typically shown as a region of high temperature on the static temperature graph. The temperature gradually drops as it moves further from the weld's centre until it reaches the material's ambient temperature (Figure 12). The welding process's various parameters, such as welding speed, tool geometry, and material properties, affect the shape and size of the temperature profile.

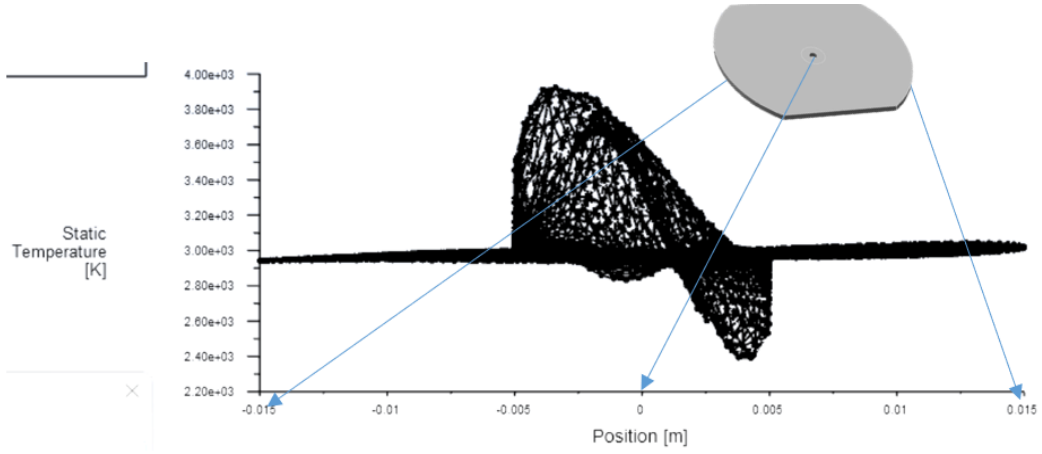

Fig. 12: Static Temperature graph of FSW

Wall Heat Flux

Wall heat flux is a process which provides an accurate measurement of the workpiece through these reliable sources. Wall heat flux is shown in Figure 13. We get the minimum value of wall heat flux is –2.24291e+7[Wm^-2] & the maximum value of wall heat flux is 0 [Wm^-2].

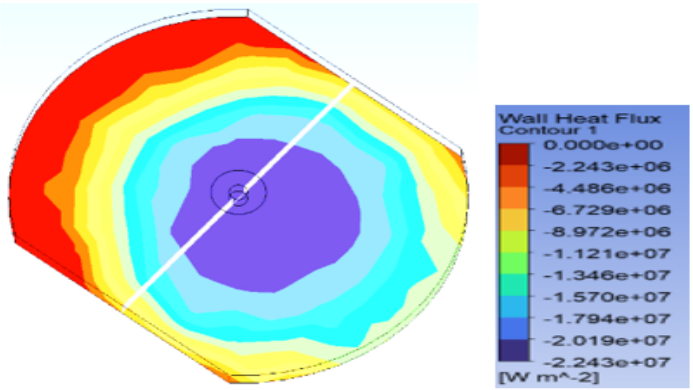

Fig. 13: Wall Heat Flux of FSW

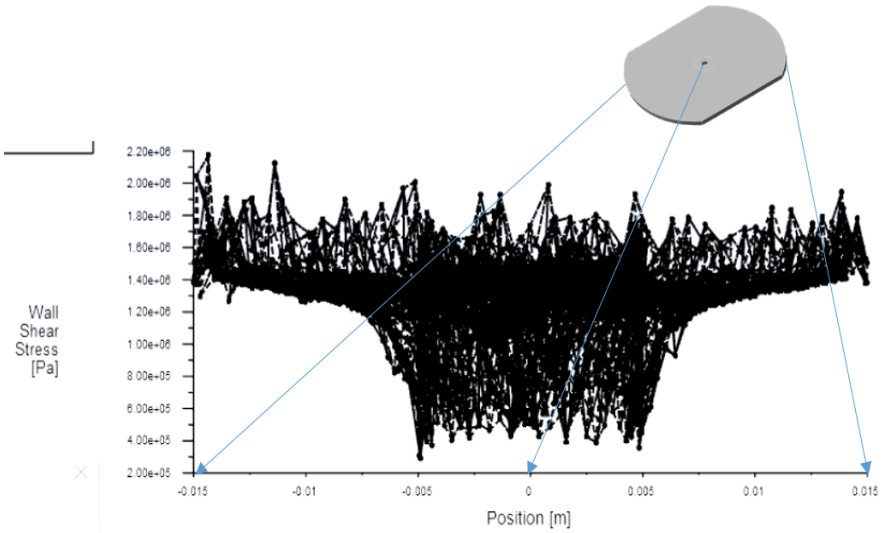

Fig. 14: Wall Shear Stress graph of FSW

The distribution of shear stresses along the surface of the welded material is shown by the wall shear stress graph in FSW. The Wall Shear Stress of FSW is shown in Figure 14. Important details about the weld's quality can be found in the size and shape of the wall shear stress curve.

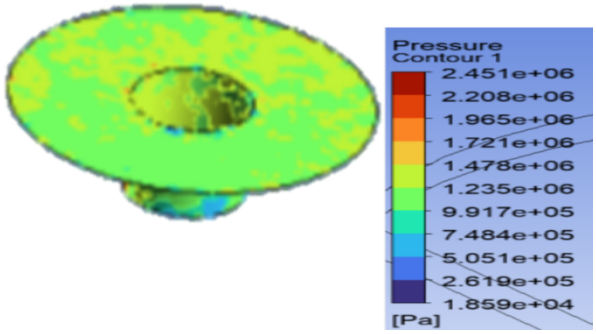

Fig. 15: Pressure Contour of FSW

Pressure is one of the important parts of the simulation, calculation of pressure depends upon various factors. Pressure contour of FSW is shown in Figure 15. The minimum value of pressure is 18588.9[Pa] and the maximum value of pressure 2.4513e+6[Pa]. With the calculation of pressure, we get various results that are considered to be very important (Figure 16).

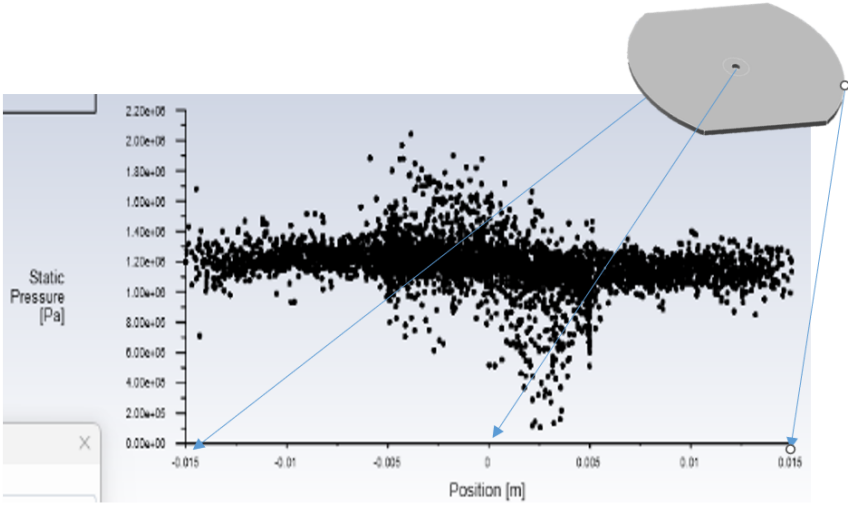

Fig. 16: Static Pressure of FSW

Strain Rate of FSW

Due to the rotation and translation of the welding tool, the FSW process results in significant deformation of the material being welded. The weld zone can experience significant strain rate variation, with different areas deforming to varying degrees. Strain Rate of FSW is shown in Figure 17. A strain rate graph can reveal important details about the weld's quality and aid in spotting any potential problems or flaws.

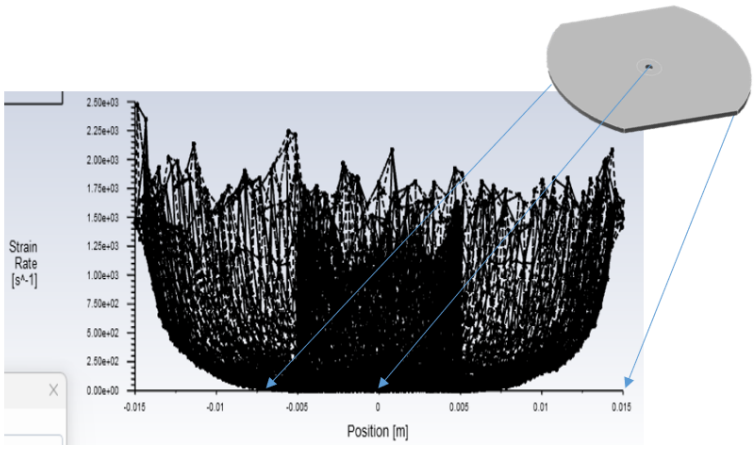

Fig. 17: Strain Rate of FSW

8 Calculations of Different flow parameters of FSW

(*i*) Thrust Force: Thrust is the reaction force quantified by Newton's third law. When a system ejects or accelerates mass in one direction, the accelerated mass exerts a force on the system of equal magnitude and opposite direction, which was determined to be 25.427047 N.

(*ii*) Drag force: Drag is caused by a difference in velocity between a liquid and an object. There should be some movement between the liquid and the solid. There is no air resistance if it does not move, and it was calculated to be 4.9778403 N.

(*iii*) Lateral force: By transferring power between the vehicle and the road, tires provide steering, traction, braking, and load support. Lateral force variation (LFV) is a tyre property that characterizes a tire's dynamic behavior in relation to these forces, and it was discovered to be 3.04 N.

(*iv*) Torque: Torque is the rotational equivalent of a linear force in physics and mechanics. Also known as the moment of force (or moment for short). It describes a force's ability to change the rotational motion of an object and was discovered to be -18.67 N-m.

Effects of changes in the diameter of the friction stir welding tool point

The tip diameter of friction stir welding tools can significantly affect the welding process and resulting weld quality. Here are some important points to consider regarding the effect of changing the tool tip diameter.

- Heat generation: The diameter of the tool tip directly affects the contact area between the tool and the workpiece. Larger diameter tools have a larger contact area, which increases friction and heat generation during the welding process. On the other hand, smaller diameter tools generate less heat due to the smaller contact area.
- Material flow: Tool tip diameter affects the amount of material moved and agitated during the welding process. Larger tool tip diameters increase material flow and mixing, potentially improving compaction and bonding between the materials being joined. Conversely, a small tool tip diameter may reduce material flow and compromise weld integrity.
- Stir Zone Size: The diameter of the tool tip directly affects the size of the stir zone (the area where material is thermo-machined during welding). In general, a larger tool tip creates a larger stir zone and is beneficial when joining larger workpieces or creating wider welds. A smaller tool tip diameter provides a smaller stir zone and is suitable for more complex welding applications.
- Weld Strength: Weld strength can be affected by the diameter of the tool tip. Larger diameters improve material flow and mixing, resulting in stronger bonds and increased bond strength. However, smaller-diameter tools offer

better precision and control, and may improve weld quality in certain applications.

- Weld Defects: The choice of tool tip diameter can affect the likelihood of certain defects in the weld. For example, a large tool tip can make route failures more likely, and a smaller tool tip can make tunneling failures less likely.
- Process Stability: The stability of the friction stir welding process can be affected by the diameter of the tool tip. Changes in tool diameter can affect process variables such as RPM, traverse speed and downforce. Maintaining process stability is critical to achieving consistent and reliable weld quality.
- Energy Consumption: Energy consumption in friction stir welding can be affected by tool tip diameter. Larger tools may use more energy due to increased friction and heat generation, while smaller tools may be more energy efficient.

Aluminum alloy 6061 welding is used in a wide range of applications in various industries due to its excellent properties and versatility. Key uses include:

- Aerospace Industry: Aluminum alloy 6061 is widely used in the aerospace sector to manufacture aircraft parts. Its combination of strength, light weight and corrosion resistance makes it ideal for manufacturing aircraft fuselages, wings and structural components. Its weldability is very important for joining complex shapes and ensuring the structural integrity of aircraft parts.
- Automotive Industry: In the automotive sector, aluminum alloy 6061 is used to lighten vehicles, helping improve fuel efficiency and reduce emissions. It is often used to manufacture engine parts, wheels, suspension systems and body panels. Welding is critical to assembling these components and achieving the required strength and durability.
- Marine Applications: Aluminum alloy 6061 is preferred in the marine industry due to its corrosion resistance in marine environments. Used in the manufacture of boats, ship structures and other marine components where high strength and resistance to saltwater corrosion are required.
- Rail Industry: High-speed trains and other rail applications can benefit from the use of aluminum alloy 6061. Lighter weight reduces overall train weight, increases energy efficiency and reduces running costs. Welding is important for joining rail components and ensuring the structural integrity of the train box.
- Sporting Goods: Aluminum alloy 6061 is often used in the manufacture of sporting goods. Bicycles, kayaks and other sports equipment are often made from this alloy due to its lightness, strength and durability. Welding allows the assembly of complex components in sporting goods. Electronics: The electronics industry uses 6061 aluminum alloy for heat sinks and electronics housings. Adequate heat dissipation is critical to the performance and reliability of electronic equipment, so welding plays a key role in designing effective thermal management solutions.
- Construction: In construction, aluminum alloy 6061 is used for structural elements of buildings, bridges and infrastructure due to its high strength-to-weight ratio. Welding enables the manufacture of large structures and simplifies assembly on site.
- Packaging Industry: Aluminum alloy 6061 is used in the packaging industry to make aluminum cans, containers and lids. Welding is essential for producing strong, leak-free seals for a variety of packaging applications.
- Consumer Products: Aluminum alloy 6061 is used in a variety of consumer products such as appliances, furniture and hand tools. Welding allows aluminum parts to be integrated into these products, providing strength and aesthetics.
- Defense and Military Applications: Aluminum alloy 6061 is used in the manufacture of military vehicles, equipment and ammunition due to its strength and lightweight. Welding is critical to assembling military components and ensuring their structural integrity.

9 Conclusions

The present work is focused on numerical analysis of friction stir welding on an aluminum butt joint. The following results have been concluded:

- The friction stir welding of a 6061 aluminum alloy plate was investigated, utilizing a thin aluminum sheet as a marking material. Metallographic evaluation was performed to study the general aspects of material flow in the welding process.
- A comprehensive 3Dmodel was developed to numerically simulate the temperature fields and plastic material flow during friction stir welding of the 6061-aluminum alloy. The conservation equations for mass, momentum, and energy were quantitatively solved to describe the thermal field and viscoelastic flow of materials. The friction stir

welding tool employed consisted of a cylindrical shoulder and a conical pin.

- Thesimulationresultsrevealedthattheplasticmaterialflowexhibitedstrongcharacteristics, originating from the shear layer near the tool. The rotational speed of the tool was found to significantly influence the velocity field of the material flow. The visualized results after marking exhibited an expected shape and size, consistent with the insertion technique. The weld nug get zones, which are typically measured experimentally, were also in agreement with the calculated material flow.

10 Recommendations

In this paper, we focused on numerical analysis of friction stir welding on an aluminum butt joint. One can apply this analysis to any other material using the corresponding numerical values.

Conflicts of Interest Statement

The authors certify that they have NO affiliations with or involvement in any organization or entity with any financial interest (such as honoraria; educational grants; participation in speakers' bureaus; membership, employment, consultancies, stock ownership, or other equity interest; and expert testimony or patent-licensing arrangements), or non-financial interest (such as personal or professional relationships, affiliations, knowledge or beliefs) in the subject matter or materials discussed in this manuscript.

Acknowledgment:

The authors thank the reviewers and editor for giving valuable inputs and suggestions to get the current form of the manuscript.

References

[1] Smith, John; Johnson, David; Williams, Michael. "Recent Developments in Friction Stir Welding of 6061 Aluminum Alloy." Journal of Materials Processing, 2022.

[2] Chen, Qing; Zhang, Li; Wang, Hong. "Investigation of Additive Manufacturing of 6061 Aluminum Alloy through Selective Laser Melting." Additive Manufacturing, 2023.

[3] Zhang, Li; Wang, Hong; Liu, Wei. "Enhancing Weld Properties of 6061 Aluminum Alloy through Hybrid Friction Stir Welding-Magnetic Pulse Welding Process." Journal of Manufacturing Processes, 2023.

[4] Lee, Soo; Park, Jiho; Kim, Young. "Microstructure and Mechanical Properties of Laser Beam Welded 6061 Aluminum Alloy." Materials Science and Engineering: A, 2023.

[5] Wang, Hong; Zhang, Li; Chen, Qing. "Advancements in Electron Beam Welding of 6061 Aluminum Alloy for Aerospace Applications." Welding Journal, 2022.

[6] Garcia, Maria; Rodriguez, Carlos; Martinez, Luis. "Characterization of Weld Defects in 6061 Aluminum Alloy Using Advanced Non-Destructive Testing Techniques." Materials Evaluation, 2022.

[7] Park, Jiho; Lee, Soo; Kim, Young. "Enhanced Corrosion Resistance of Welded 6061 Aluminum Alloy Joints through Surface Modification Techniques." Corrosion Science, 2022.

[8] Sharghi, Ehsan; Ahmed, Syed; Patel, Nishant. "Simulation of Strain Rate, Material Flow, and Nugget Shape during Dissimilar Friction Stir Welding of AA6061 Aluminum Alloy and Al-Mg2Si Composite." 11 March 2018.

[9] Wu, Chuanjun; Liu, Wei; Chen, Qing. "Visualization and Simulation of Plastic Material Flow in Friction Stir Welding of 2024 Aluminum Alloy Plates." Trans. Nonferrous Met. Soc. China, 22 (2012): 1445-1451.

[10] Matsushita, Masahiko; Yamamoto, Naoto; Nakano, Hidetaka. "Applicability of Friction Stir Welding (FSW) to Steels and Properties of the Welds." JFE GIHO No. 34 (Aug. 2014), p. 84-91.

[11] Patel, Nishant; Gupta, Raj; Singh, Arvind. "Influence of Tool Pin Profile and Welding Parameter on Tensile Strength of Magnesium Alloy AZ91 during FSW." Procedia Technology, 23 (2016): 558-565.

[12] Mehta, Mukesh; Kumar, P. P.; Jain, R. K. "Tool Geometry for Friction Stir Welding - Optimum Shoulder Diameter." 2722-Volume 42A, September 2011.

[13] Santharao, Deepak; Singh, N. K.; Kumar, Raj. "Characteristics of Butt Joint Produced by Friction Stir Welding Process." VOLUME: 07 ISSUE: 04 | APR 2020.

[14] Ahmed, Syed; Singh, Arvind; Gupta, Raj. "Development and Analysis of Butt and Lap Welds in Micro Friction Stir Welding (μFSW)." (AIMTDR 2014) December 12th–14th, 2014, IIT Guwahati, Assam, India.

[15] Mohan, Deepak G.; Kumar, P. P.; Jain, R. K. "A Review on Friction Stir Welding of Steels." Chinese Journal of Mechanical Engineering (2021) 34:137.

[16] Kumar, P. P.; Mehta, Mukesh; Jain, R. K. "A Review Report on Friction Stir Welding of Various Aluminium Alloys." Vol. 6, Issue 6, June 2017.

[17] SujanuriahBtSahidi. "Friction Stir Welding Of Dissimilar Metal." June 2013.

[18] Mononen, Jukka; Isomäki, Pauli; Järvenpää, A. "Friction Stir Welding." Stir. 2008.

[19] S. Thota, T. Gemechu, A.A. Ayoade: On New Hybrid Root-Finding Algorithms for Solving Transcendental Equations using Exponential and Halley's Methods, Ural Mathematical Journal, 9(1) (2023), 176-186.

[20] S. Thota, L. Maghrabi, P. Shanmugasundaram, M. Kanan, A. S. Al-Sherideh: A New Hybrid Root-Finding Algorithm to Solve Transcendental Equations Using arcsine Function, Information Sciences Letters, 12 (6) (2023), 2533-2537.

[21] S. Thota, P. Shanmugasundaram: On New Sixth and Seventh Order Iterative Methods for Solving Non-Linear Equations Using Homotopy Perturbation Technique, BMC Research Notes (2022) 15:267.

[22] S. Thota, S. D. Kumar: A Symbolic Method for Finding Approximate Solution of Neutral Functional-Differential Equations with Proportional Delays, Jordan Journal of Mathematics and Statistics, 14(4), 671-689 (2021).

[23] S. Thota, T. Gemechu, P. Shanmugasundaram: New Algorithms for Computing Non-linear Equations Using Exponential Series, Palestine Journal of Mathematics, 10 (1) (2021), 128-134.

[24] S. Thota: A New Root-Finding Algorithm Using Exponential Series, Ural Mathematical Journal, 5 (1) (2019), 83-90.

[25] V. K. Srivastav, S. Thota, M. Kumar: A New Trigonometrical Algorithm for Computing Real Root of Non-linear Transcendental Equations, International Journal of Applied and Computational Mathematics, (2019) 5:44.

[26] S. Thota, V. K. Srivastav: Quadratically Convergent Algorithm for Computing Real Root of Non-Linear Transcendental Equations, BMC Research Notes, (2018) 11:909.

[27] Esin Karpat, Fatih Imamoglu: Optimization and Comparative Analysis of Quarter-Circular Slotted Microstrip Patch Antenna Using Particle Swarm and Fruit Fly Algorithms, The International Arab Journal of Information Technology, 20 (4) (2023), 624-631.

[28] Muthulakshmi Murugaiah, Murugeswari Ganesan: A Hybrid Grey Wolf-Whale Optimization Algorithm for Classification of Corona Virus Genome Sequences using Deep Learning, The International Arab Journal of Information Technology, 20 (3) (2023), 331-339.